Microstructure and mechanical behavior of AlSiCuMgNi piston alloys reinforced with TiB_2 particles

D. G. ZHAO*, X. F. LIU, Y. C. PAN, Y. X. LIU, X. F. BIAN
The Key Laboratory of Materials Liquid Structure and Heredity, Ministry of Education, Shandong University, Jinan 250061, People's Republic of China
E-mail: degang2008@163.com

Published online: 15 May 2006

AlSiCuMgNi piston composites reinforced with *in-situ* TiB_2 particles were fabricated by mixing salts reaction process successfully. Microstructures of the composites were observed by mean of scanning electron microscope (SEM) and transmission electron microscope (TEM). X-ray diffraction (XRD) was used to identify the phases in the composites. TiB_2 reinforcement grows in equiaxed or near equiaxed shape and the interfaces between reinforcements and matrix are clear. Compared with the matrix alloys, the composites show an obvious aging peak and an incubation time in the hardness. The aging is accelerated in the composites reinforced with TiB_2. At room temperature, the ultimate tensile strength (UTS) of the composites increases as the percentage of TiB_2 reinforcement increases. When the temperature is beyond 250°C, the ultimate tensile strength of the piston composites decreases sharply. The fracture surfaces of the piston composites are analyzed.

1. Introduction

Metal matrix composites (MMCs) are being explored because of their superior properties compared with those of most conventional metal materials. The main reinforcing phases include whiskers, short fibers and ceramic particles. During the last three decades, a few of whiskers, short fibers or particulate reinforced aluminum matrix composites have extensively studied and successfully used in the automobile industry [1–4]. More recently, particulate reinforced metal matrix composites (PRMMCs) have been the subject of numerous research works due to their ease of fabrication, lower costs and isotropic properties. The conventional ex-situ PRMMCs are fabricated by directly adding reinforcements into its matrix. Recently, an *in-situ* technique has been developed [5, 6]. *In-situ* synthesizing of PRMMCs involves the production of reinforcements within the matrix during the fabrication process [7, 8]. This technology offers an attractive set of features: clean interface, fine reinforcements and economical process. Several *in-situ* technologies have emerged in the past two decades such as self-propagation high-temperature synthesis (SHS) [9], exothermic dispersion (XD) [10], reactive gas injection (RGI) [11], and mixing salt reaction [12] etc.

TiB_2 particles are one of the best reinforcements because of their high melting point (2790°C), high hardness (960 HV) and high modulus (530×10^3 GPa). Furthermore, in contrast to most ceramics, it is electrical and thermal conductive [13]. At present, there are many papers about AlSiCuMgNi piston alloy reinforced with the short fibers. Investigation about piston composites reinforced with TiB_2 particles, however, is limited. In this study, the AlSiCuMgNi piston composites reinforced with TiB_2 particles were fabricated by mixing salts reaction process. Compared with the unreinforced matrix alloys, the aging behavior of the composites was studied. The tensile tests were tested to evaluate the effect of percentage of TiB_2 particles on mechanical properties of the composites at room and elevated temperature. Furthermore, the fracture behavior of the piston composites was studied by the fracture surface analyses.

2. Experimental

The MMCs in this study were fabricated by mixing salts reaction process at 860°C using KBF_4 and K_2TiF_6 salts. The compositions of the matrix piston alloys used in the paper are listed in Table I.

*Author to whom all correspondence should be addressed.
0022-2461
DOI: 10.1007/s10853-006-6247-y

TABLE I Chemical compositions of the matrix piston alloys (wt.%)

Matrix alloy	% Si	% Cu	% Mg	% Ni	% Al
Alloy1	11.80	1.10	1.10	0.96	Balance
Alloy2	13.20	4.50	1.12	0.94	Balance

The matrix alloy melt was prepared in a clay-graphite crucible using an intermediate frequency furnace and kept at 860°C. A pre-weighted mixture of KBF_4 and K_2TiF_6, with an atomic ratio of Ti/B = 1:2, was added into the melt using a stirring method. Then, the melt was stirred for 10–15 min and poured after the slag was cleared. Refining and modifying treatments were needed by DSG (degassing flux) and Al-P master alloy [14].

The samples for microstructure observations and X-ray diffraction analysis were cut from the composite samples. The microstructures of the polished samples were examined with scanning electron microscope (SEM). The characters of the reinforcements were examined using an H-800 (200 KV) transmission electron microscope (TEM). To study the age behavior, all samples were treated in the following way: solution treatment at 510°C for 6 h, water quenching at 60°C and isothermal aging for various time at 200°C. The microhardness of all samples was tested using Vickers Hardness Tester. The ultimate tensile strength (UTS) specimens, with 6 mm gauge diameter and 25 mm gauge length, were machined from the composite samples. Heat-treatment was performed under T6 conditions to achieve maximum mechanical properties. Tensile tests were used to evaluate the mechanical properties of the composites at both the room temperature and elevated temperature. Tensile tests were carried out in accordance with ASTM E8 and the strain rate for tensile test was 0.005 mm s^{-1}. Four tensile specimens were tested at each condition and the reported results are average values. Fracture surfaces of tensile specimens were analyzed by the SEM.

3. Results and discussion

3.1. Phase identification and microstructures

The X-ray diffraction (XRD) pattern of 2% TiB_2/Alloy1 composites is shown in Fig. 1. It indicates that the present phases in the composites include α-Al, β-Si and iB_2, while no other discernible diffraction peaks appear. The result of the XRD analysis confirms that Al matrix piston composite reinforced with TiB_2 can be fabricated by common casting technique utilizing the mixing salts reaction.

The shape, size and spatial distribution of the *in-situ* reinforcements profoundly affect the mechanical properties of the composites. Fig. 2 shows the SEM micrographs of 2%TiB_2/alloy1 composites. It can be found that the reinforcements distribute uniformly in the matrix alloy. Connected with the result of XRD, the EPMA indicates that the near-equiaxed reinforcements are TiB_2 particles. From the Fig. 2c, it can be observed the TiB_2 particles are mostly less than 1 μm in size, which distribute uniformly around the primary silicon and their interfaces are very clean.

TABLE II Results of aging behavior for the matrix alloys and the 2%TiB_2/alloy composites

	HV								
Sample	0 h	2 h	4 h	6 h	8 h	10 h	12 h	14 h	16 h
Alloy 1	71	82	86	78	86	95	92	90	90
2% Tib_2/Alloy 1	90	102	85	83	112	108	107	107	107
Alloy 2	80	83	87	90	86	98	95	95	95
2% Tib_2/Alloy 2	101	130	108	106	134	129	130	130	130

Fig. 3a reveals a typical bright field TEM image and respective selected area diffraction pattern of the TiB_2. It shows that the TiB_2 particle is hexangular and near-equiaxed shape. Fig. 3b also exhibits the interfaces between the TiB_2 particle and matrix are very clean and there is no interfacial reaction. The shape of the reinforcements is related to their crystal structures. TiB_2 has a C32-AlB_2 structure with lattice parameter $a = 0.3028$ nm and $c = 0.3228$ nm. The crystal structure of TiB_2 shows high geometrical symmetry for the chemical bond between the atoms Ti and B. This indicates that TiB_2 will grow at almost the same speed in each direction and form equiaxed or near equiaxed shape.

3.2. Aging behavior

The introduction of reinforcement phases into the piston alloy can significantly alter the nucleation and growth kinetics of precipitation in the matrix. So the aging characteristic can be influenced by those changes in the precipitation of the matrix. Table II shows the results of aging behavior for the matrix alloys and the composites. It can be seen that the hardness of composites reinforced with TiB_2 is higher than those of the matrix alloys. As the aging time increases, the hardness of unreinforced matrix alloys increases slowly and incubation time is not obvious. In contrast to the unreinforced matrix alloys, the TiB_2/alloy composites show an obvious incubation time in the hardness. The hardness of TiB_2/alloy composites first increases and reaches a peak, and then decreases. After an incubation time, the hardness increases again and reaches the maximum, and then tends to be constant.

In similar studies, many investigators reported accelerated aging kinetics about composites reinforced with SiC or Al_2O_3 particulates, whereas Kim reported the suppression in aging kinetics of composites reinforce with SiC whiskers [15–17]. Table II shows that the aging peaks of 2%TiB_2/Alloy1 and 2%TiB_2/Alloy2 are at 8 h, while those of the matrix alloys are at 10 h. The aging peaks of composites are shifted to an earlier time than the matrix alloys. The phenomenon is due to the changes in the precipitation of the matrix. The difference in thermal expansion coefficient between the TiB_2 and the matrix is so large, that even a small change in

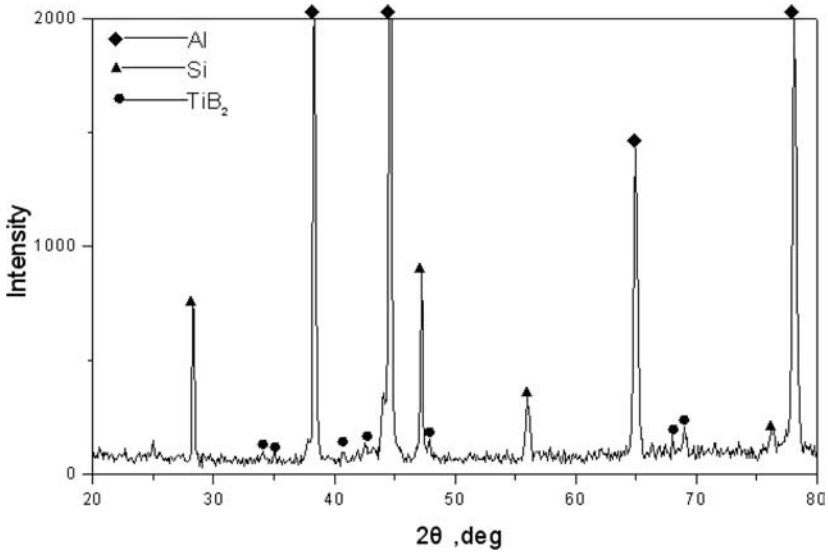

Figure 1 X-ray diffraction pattern of 2%TiB_2/alloy1 composites.

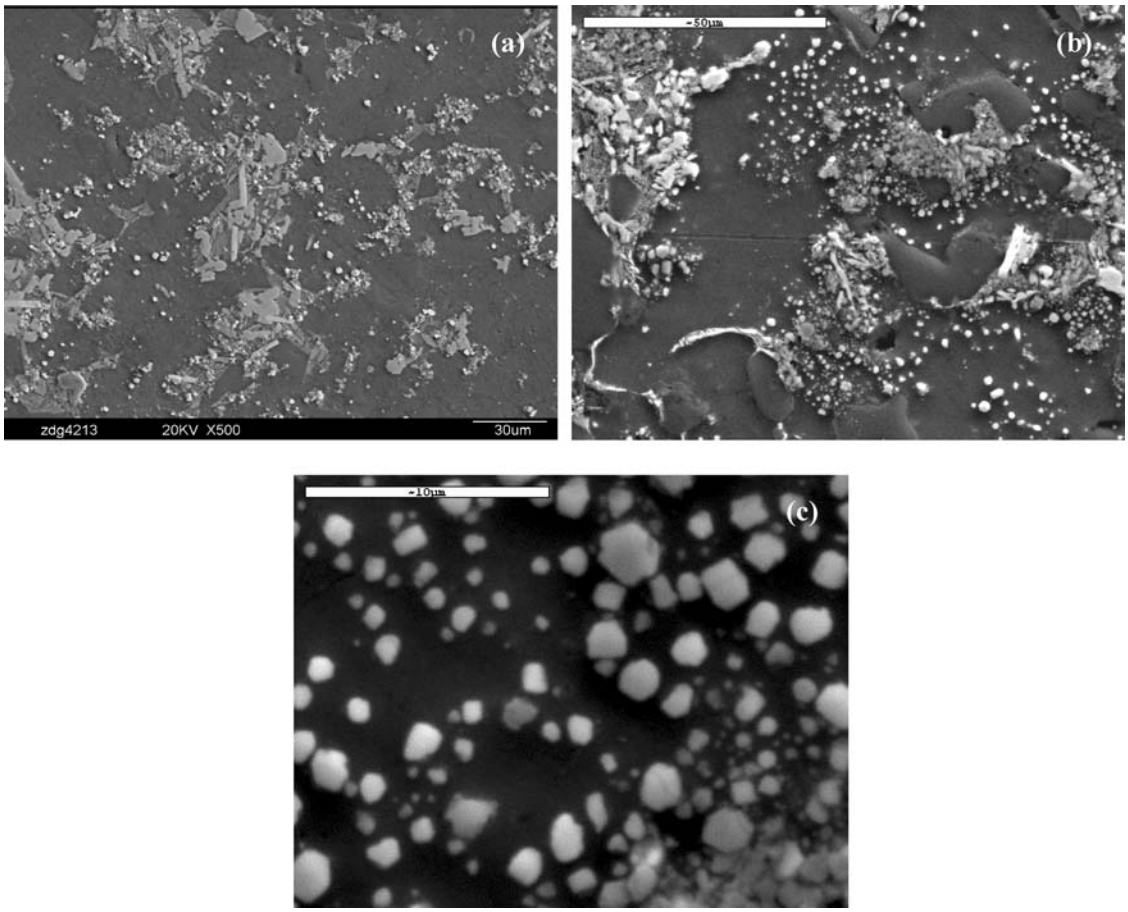

Figure 2 SEM micrographs of 2%TiB_2/alloy1 composites: (a) Magnification of 500; (b) magnification of 1000; (c) morphologies of TiB_2.

temperature will generate thermal residual stress in the matrix. So the composites reinforced with TiB_2 have the higher dislocation density than the unreinforced matrix alloys. Those dislocations can serve as the sites for the nucleation of strengthening precipitation such as Mg_2Si, AlCuMg. As a result, the nucleation of strengthening precipitation in the matrix is altered and the "shift of aging peak" phenomenon appears.

3.3. Tensile properties

The tensile properties of the unreinforced matrix alloys and the TiB_2/alloy composites with 2, 4 and 6 wt.% TiB_2

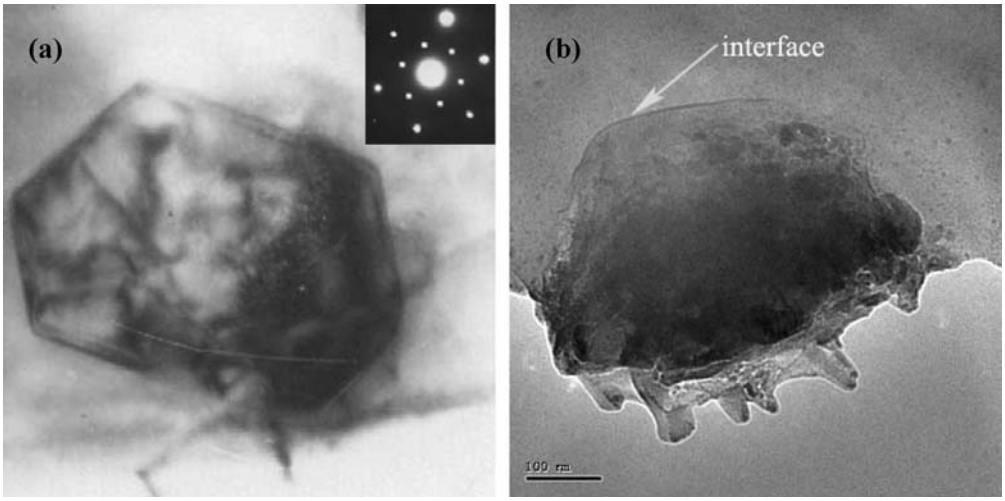

Figure 3 TEM micrographs (a) bright field TEM image and respective SAD of TiB_2 (b) image showing the clean interface between the matrix and TiB_2.

are listed in Table II. It can be found that the UTS of the TiB_2/alloy composites at room temperature increases as the percentage of TiB_2 increases. For example, the UTS of 6%TiB_2/alloy1 composite increases by 55% compared to that of the unreinforced matrix alloy1. The UTS of the 6%TiB_2/alloy2 is 341.6 MPa, which is 43.2% higher than that of the unreinforced matrix alloy2. Compared with the TiB_2/alloy1, the UTS of the TiB_2/alloy2 is higher because alloy2 have a higher content of Cu. In addition, the elongation value of the TiB_2/alloy composites decreases as the percentage of TiB_2 increases. This decrease corresponds to the decrease in pile-up spacing due to the increase in the percentage of TiB_2 reinforcements.

The prime reason for the resulting strengthening is due to the grain refinement. Lakshmi [18] have corroborated that the introduction of *in-situ* TiB_2 in α-Al can result in the decrease of the grain size. According to Hall-Petch equation,

$$\sigma_y = \sigma_0 + kd^{-1/2}$$

where σ_y is Yield Strength, d is grain size, k is a constant, Yield Strength of composites is enhanced because of the grain refinement. Another reason is due to the presence of a number of the appending dislocations around the TiB_2 particles because of the difference of coefficient of thermal expansion (CTE) between the matrix and TiB_2 particles.

Table IV lists the tensile properties of the matrix alloys and 2%TiB_2/Alloy composites at elevated temperatures. From Table IV, it is clear that the strength of 2%TiB_2/Alloy composites decreases slowly as the temperature increases from 300 K to 523 K. When the temperature is higher than 523 K, the UTS decreases sharply. At 623 K, the UTS of 2%TiB_2/alloy1 composite and 2%TiB_2/alloy2 composite is 58.5 MPa and 65.6 MPa respectively.

The fracture surfaces of 2%TiB_2/alloy2 composite are shown in Fig. 4. Some dimples which are associated with ductile fracture of matrix and a few of pulled out particulates, are found from the Fig. 4a. However in Fig. 4b, some relatively flat and smooth regions, which are called mirror regions, are observed. Emergence of mirror regions means that the composites exhibit a transgranular cleavage mechanism microscopically. So the fracture surfaces show a ductile failure macroscopically and brittle failure microscopically.

Fig. 5 shows the fracture surfaces of the TiB_2/alloy2 composites with mass fraction of about 2 and 6% at 623 K. Similar fracture surfaces were also observed in the TiB_2/alloy1composites. These indicate that the tensile fracture surfaces of the piston composites with different mass fraction of TiB_2 are quite different at high temperature. As the percentage of TiB_2 particles increases, the mirror regions increase and the composites show an obvious decrease in ductile. In addition, compared with the fracture surfaces of TiB_2/alloy2 composite at room temperature, the larger and deeper dimples are observed in the fracture surface of TiB_2/alloy2 composite at room temperature, the larger and deeper dimples are observed in the fracture surfaces of TiB_2/alloy2 composite at 623 K.

Traditionally, most researchers assumed that fracture in PRMMCs follows the sequence: void nucleation at

TABLE III Tensile properties of the matrix alloys and TiB_2/alloy composites at room temperature.

Sample	UTS (Mpa)	0.2% Yield strength (Mpa)	Elongation (%)
Alloy 1	206.8	162.5	5.4
2%TiB_2/Alloy 1	287.1	221.7	5.0
4%TiB_2/Alloy 1	302.5	245.6	4.2
2%TiB_2/Alloy 1	320.5	251.2	3.8
6%TiB_2/Alloy 1	231.2	171.6	4.9
Alloy 2	307.8	260.5	4.5
2%TiB_2/Alloy 2	332.5	271.3	3.9
6%TiB_2/Alloy 2	341.6	278.6	3.7

TABLE IV Tensile properties of the matrix alloys and 2%TiB_2/Alloy composites at elevated temperatures

	300 K		423 K		523 K		623 K	
Sample	UTS(MPa)	δ (%)	UTS(MPa)	δ (%)	UTS(MPa)	δ (%)	UTS(MPa)	δ (%)
Alloy 1	206.8	5.2	180.5	5.4	168.3	6.4	52.4	8.7
2%TiB_2/Alloy 1	287.1	5.4	223.6	5.6	201.5	6.2	68.2	8.5
Alloy 2	231.2	4.9	186.2	5.2	170.4	6.2	56.8	8.2
2%TiB_2/Alloy 2	307.8	4.5	253.1	4.8	210.5	5.8	71.54	7.9

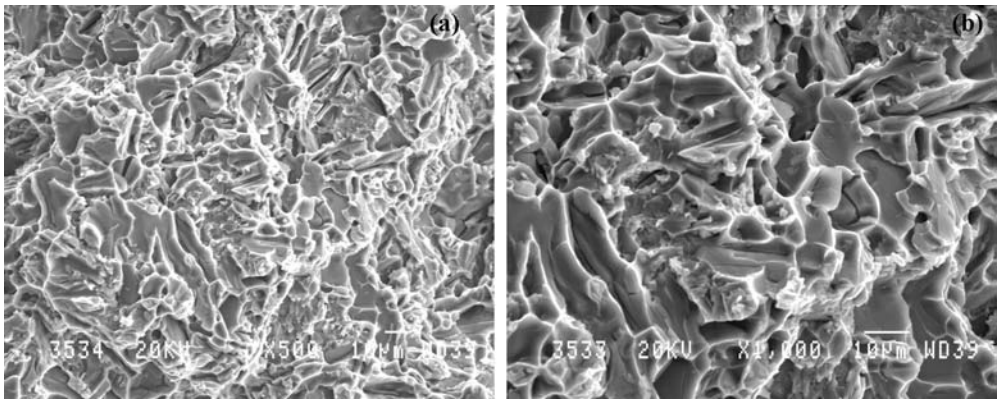

Figure 4 Fracture surfaces of the 2%TiB_2/alloy2 composite at room temperature. (a) Magnification of 500; (b) magnification of 1000.

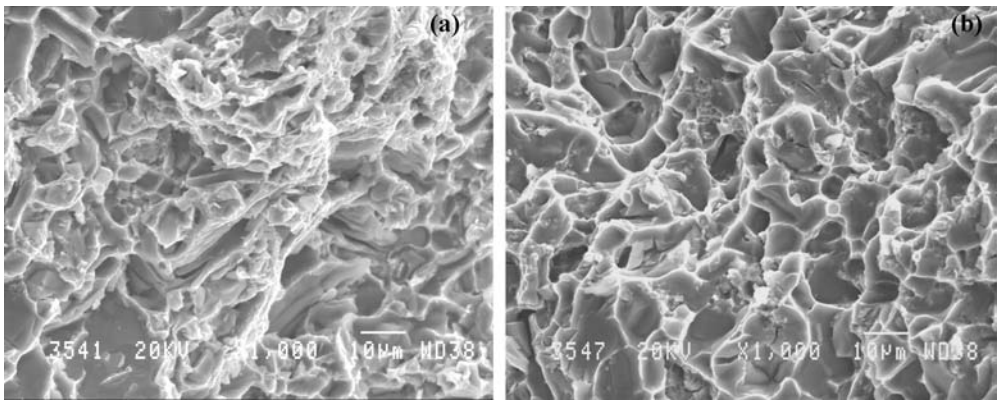

Figure 5 Fracture surfaces at 623 K for the TiB_2/alloy2 composites with mass fraction of (a) 2%, (b) 6%.

second phase particles followed by failure in the matrix through void coalescence. Such as SiCp/Al composite, it can be easily found particle cracking [19, 20]. However, the size of the SiC reinforcements in the privious researches is larger than 10 μm. In fact, the size of reinforcement has an important influence on the void nucleation. As the TiB_2 particles are mostly less than 1 μm in size and no particle cracking is found in this study, it is concluded that void nucleation of fracture behavior in the TiB_2/alloy piston composites is related to the interfacial bonding strength between the TiB_2 reinforcements and matrix. More research about it is needed in future.

4. Conclusions

The microstructure and mechanical properties of AlSiCuMgNi piston composites reinforced with TiB_2 particles were studies. The following conclusions were obtained.

(1) TiB_2 reinforcements distribute uniformly in the matrix. TiB_2 grows in equiaxed or near equiaxed in shape. The interfaces between the TiB_2 and matrix are clean and there is no interfacial reaction.

(2) Compared with the unreinforced matrix alloys, the piston composites reinforced with TiB_2 show an obvious aging peak and an incubation time in the hardness. The aging peaks of the piston composites are shifted to an earlier time than the unreinforced matrix alloys.

(3) At room temperature, the UTS of piston composites reinforced with TiB_2 increases as the percentage of TiB_2 reinforcements increases. When the temperature is higher than 523 K, the UTS of piston composites decreases sharply.

Acknowledgments

The authors are very grateful for the support of National Natural Science Foundation of China (No. 50171037), and the support of the Key Project of Science and Technology Research of Ministry of Education of China (No. 01105).

References

1. B. MARUYAMA and W. H. HUNT, *J. Organomet. Chem.* **51** (1999) 59.
2. M. V. KEVORKIJAN, *Am. Ceram. Soc. Bull.* **59** (1998) 53.
3. M. FUJINE and M. YAMASHITA, *J. Jpn. Inst. Light Met.* **49** (1999) 564.
4. J. E. ALLISON and G. S. COLE, *J. Organomet. Chem* **45** (1993) 19.
5. G. NEITE and S. MIELKE, *Mater. Sci. Eng. A.* **148** (1991) 85.
6. W. HENNING, G. NETTE and E S. CHMID, *Metallurgist.* **38** (6) (1994) 451.
7. I. A. IBRAHIM, F. A. MOHAMED and E. J. LAVERNIA, *J. Mater. Sci.* **26** (1991) 1156.
8. D. J. LLOYD, *Inter. Mater. Rev.* **39** (1994) 23.
9. C. F. FENG and L. FROYEN, *Scripta Mater.* **36** (1997) 467.
10. Z. Y. MA, J. H. LI, M. LUO and Y. X. GAO, *Scripta Mater.* **29** (1993) 225.
11. P. SAHOO and M. J. KOCZAK, *Mater. Sci. Eng. A.* **144** (1991) 37.
12. P. DAVIES and J. SHELL, *Key. Eng. Mater.* **77** (1993) 357.
13. A. CHRYSANTHOU and G. ERBACCUIO, *J. Mater. Sci.* **30** (1995) 6339.
14. X. F. LIU, J. Q. QIAO and Y. X. LIU, *Acta Metallurgica Sinica*. **40** (2004) 471.
15. S. SURESH, T. CHRISTMAN and S. SUGIMURA, *Scripta Mater.* **23** (1989) 1599.
16. M. GUPTA, T. S. SRIVATSAN, F. A. MOHAMED and E. J. LAVERNIA, *J. Mater. Sci.* **28** (1993) 2245.
17. T. S. KIM, T. H. KIM, K. H. OH and H. L. LEE, *J. Mater. Sci.* **27** (1992) 2599.
18. S. LAKSHMI, L. LU and M. GUPTA, *J. Mater. Process. Technol.* **73** (1998) 160.
19. Q. G. ZHANG, H. X. ZHANG and M. Y. GU, *Mater. Lett.* **58** (2004) 3545.
20. M. TAYA, K. E. LULAY and D. J. LLOYD, *Acta Metallurgica Sinica* **27** (1991) 73.

Received 6 May 2005
and accepted 15 August 2005